

# Design of a Novel Tremor Suppression Device Using a Linear Delta Manipulator for Micromanipulation

Dongjune Chang, Gwang Min Gu and Jung Kim\*, *Member, IEEE*

**Abstract**—In this paper, the design of a high precision device using a Linear Delta manipulator was proposed to compensate for the tremor signal in three translational directions. A Linear Delta manipulator is a suitable tremor suppression device due to the simple structure and high stiffness with the vertical direction in the application of micro manipulation such as microsurgery and cell manipulation. In order to implement the mechanism of the Linear Delta manipulator to the device, three voice coil motors and three linear encoders with high resolution were used. The flexure mechanism was applied to the device to avoid the friction effect of the small ball joint. Finally, the experiments for the validation of the proposed device were performed as follows: (1) position control in each axis for accuracy, and (2) sine wave tracking (500  $\mu\text{m}$ , 12Hz) for bandwidth of the system.

## I. INTRODUCTION

Micro-scale positioning technology has been a primary concern in the field of micromanipulation. Of many devices that satisfy individual requirements for high precision control, there are needs for hand-held devices in order to give an operator more natural motion [1-2]. However, in case of hand-held devices, the physiological tremor of the operator can be transmitted into the device. In [2], Patkin, M revealed the physiological hand tremor fundamentally limited the accuracy of the manipulation, especially for cell-manipulation such as insertion and extraction, and could inhibit the quality and efficiency of the repetitive tasks. Also, the limb motion of the micro-surgeon can considerably degrade an operator's performance during microsurgery [3-4].

Moreover, physiological tremor occurs in small magnitude even in the case of healthy people, though it is barely recognizable to the naked eye due to the amplitude of 50 - 150  $\mu\text{m}$  in each principle axis [1]. The tremor originates from the central nervous system (CNS) and has the characteristics of the non-stationary and modulated frequency within the range of 8-12Hz. Several robotic approaches by passive suppression were performed [5-8] to reduce the magnitude of the tremor with the high frequency band compared to the frequency of voluntary motion. However, the passive suppression method was limited to fully eliminate the tremor signal, because the mechanical properties of the passive system with a person's hand and arm just played a role of a low pass filter. In this

context, many active compensation devices have been widely suggested [9]-[19].

The Micron instrument [19], a well-known active hand-held device developed by Riviere et al. [10] and Wei T. Ang et al. [9], allows effective suppression of erroneous motions of the hand during micro-surgery. The device is a successful hand-held micromanipulator that self-actuates through three piezoelectric actuators located between the handle grip and the tip of the instrument. The manipulator is a three degree of freedom (DOF) parallel manipulator and has one vertical movement and two rotational movements that meet requirements in the fields such as retinal laser photocoagulation and retinal vessel cannulation [12-14]. The ITrem instrument developed by Latt et al. [17] was nearly similar with the Micron instrument in terms of motion of mechanism of the main manipulator. Although the mentioned active platforms were developed, the design using a Linear Delta manipulator having the high stiffness and simple structure has not been proposed as a tremor suppression device.

The Linear Delta manipulator is a 3 DOF translational parallel manipulator with linear actuation [20-23]. This manipulator has the following four advantages: (1) Its kinematics allows a travel space as large as desired in one direction. The manipulator has a relatively large workspace in the direction of movement in one side of the axis. The vertical movement in microsurgery, such as the insertion, is ensured. (2) It has maximum stiffness of the z-axis directional motion. (3) It has good sensitivity in the desired direction [23]. (4) As it has same coordinate system between the base frame and end frame, it has the inherited structural property of having relatively simple kinematics and a Jacobian matrix. Very little research has been presented regarding developing a Linear Delta manipulator in manipulation applications with small scale, such as micromanipulation. Because the stiffness is required to transmit the force of the operator during the insertion task, the Linear Delta manipulator is appropriate for the task. Also, its high stiffness ensures efficiency in the vertical direction of repetitive tasks such as back-and-forth motion along the z axis direction.

The paper proposes the design of a tremor suppression device based on the Linear Delta mechanism, which is applicable to micromanipulation to compensate for the tremor signals in the three translational directions. We implemented three voice coil motors with high resolution encoders to the actuating parts of the device to ensure the workspace and resolution of the motion. And a flexure mechanism was applied to the spherical joint parts of the device to avoid friction effect of the use of small ball joint. This paper is organized as follows. Section II summarizes the requirements of the device and describes the design of the manipulator as a

D.J. Chang is with the Dongbu Robot Co., Ltd, Gyeonggi-do, 420-734, Korea (phone: +82-32-329-5551(540), fax: +82-32-329-5483; e-mail: dongjune.chang@dongbu.com)

G.M.Gu is with the Department of Mechanical Engineering, Korea Advanced Institute of Science and Technology (KAIST), Daejeon, 305-701, Korea, (e-mail: friendgoos@kaist.ac.kr)

J. Kim is with the Department of Mechanical Engineering, Korea Advanced Institute of Science and Technology (KAIST), Daejeon, 305-701, Korea (phone: +82-42-350-3231; fax: +82-42-350-5230; email: jungkim@kaist.ac.kr)

tremor suppression device. Section III presents the experimental results of the position control of the device as a feasibility test. Finally, Section IV discusses and concludes about the proposed system.

## II. METHODS & MATERIALS

As the tremor suppression system, the manipulator can operate active compensation in the anti-phase of tremulous signals. Hence, the design of the manipulator was considered for the requirements; the ability to track the linear combination of the sinusoidal signals with frequency range of 8-12 Hz, amplitudes of 50-150  $\mu\text{m}$ , and accuracy of 10  $\mu\text{m}$ . Because the task direction of micro-manipulation is the insertion direction of the tool, the end-effector should have large workspace along the z axis. The Linear Delta mechanism was appropriate to meet the requirements mentioned above.

### A. Linear Delta parallel mechanism

The Linear Delta mechanism was suggested as a one of the parallel manipulators with three DOF translational motions [20]. Unlike a well-known Delta mechanism, it uses three linear actuators enabling a mobile platform, its end-effector, to three translational movements (x-y-z) with respect to its base platform. The base platform has three identically aligned linear guides in the vertical direction z. Each of these prismatic components has one slider that can move along the corresponding guide, activated by each actuator. Furthermore, all sliders contain the same kinetic chains, which connect between the mobile platform and the base platform. Each kinematic chain consists of two parallel bars with identical length  $L$  and four spherical joints at each end of the full parallel bars. All notations and equations are followed by [20].

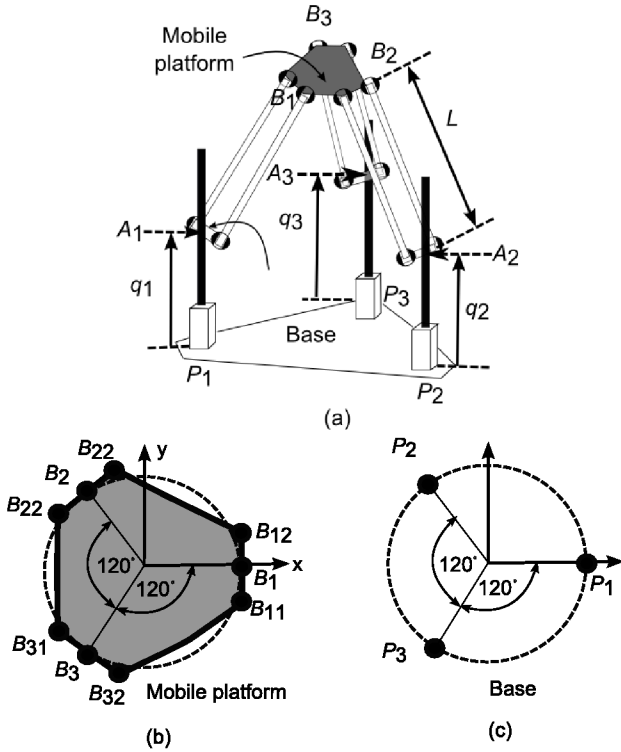


Fig. 1. (a) Schematic diagram of the Linear Delta manipulator, (b) geometric description of the mobile platform, base platform and (c) base of the Linear Delta manipulator [21]

If the control variable  $[q_1, q_2, q_3]^T$  is given, the kinematic model of the device can be easily represented to determine the pose (position and orientation) of the end-effector with respect to a reference frame  $\{R_0\}$ , which has constraint equations as follows, as shown in Fig. 1:

$$A_i B_i^2 - L^2 = 0 \text{ for } i=1, 2, 3, \quad (1)$$

where the coordinate points and in the reference frame related to the base are given by

$$\begin{aligned} [A_i]_{base} &= [R_b \cos \alpha_i, R_b \sin \alpha_i, q_i] \\ [B_i]_{mobile} &= [x + R_n \cos \alpha_i, y + R_n \sin \alpha_i, z], \end{aligned} \quad (2)$$

where  $\alpha_i = \frac{2\pi}{3}(i-1)$  for  $i=1, 2, 3$  (see the Fig. 1), and

$R_b$  and  $R_n$  indicate the radius of the base platform and mobile platform, respectively. The constraint equations can be evolved into the inverse kinematics model of the system. Then, each element of control variables  $[q_1, q_2, q_3]^T$  is formulated by

$$q_i = z + \sqrt{L^2 - (x - (R_b - R_n) \cos \alpha_i)^2 - (y - (R_b - R_n) \sin \alpha_i)^2} \quad \text{for } i=1, 2, 3 \quad (3)$$

or

$$\begin{aligned} q_1 &= z + \sqrt{L^2 - (x-d)^2 - y^2} \\ q_2 &= z + \sqrt{L^2 - (x + \frac{1}{2}d)^2 - (y - \frac{\sqrt{3}}{2}d)^2} \\ q_3 &= z + \sqrt{L^2 - (x + \frac{1}{2}d)^2 - (y + \frac{\sqrt{3}}{2}d)^2} \end{aligned} \quad (4)$$

To find the relationship between the velocity of the end-effector and the control variables, we need to derive the Jacobian matrix by differentiating (4).

$$J_x \begin{bmatrix} \dot{x} \\ \dot{y} \\ \dot{z} \end{bmatrix} = J_q \begin{bmatrix} \dot{q}_1 \\ \dot{q}_2 \\ \dot{q}_3 \end{bmatrix} \quad (5)$$

$$J_x = \begin{bmatrix} (B_1 - A_1)^T \\ (B_2 - A_2)^T \\ (B_3 - A_3)^T \end{bmatrix} = \begin{bmatrix} x-d & y & z-q_1 \\ x + \frac{1}{2}d & y - \frac{\sqrt{3}}{2}d & z-q_2 \\ x + \frac{1}{2}d & y + \frac{\sqrt{3}}{2}d & z-q_3 \end{bmatrix} \quad (6)$$

$$J_q = \begin{bmatrix} z-q_1 & 0 & 0 \\ 0 & z-q_2 & 0 \\ 0 & 0 & z-q_3 \end{bmatrix}$$

Also, as  $J_q$  is a diagonal matrix and non-singular (if guaranteed),

$$J^{-1} = J_q^{-1} J_x \quad (7)$$

To avoid singularity problems, we need to consider two types of singularities of the parallel manipulator; serial singularities ( $|J_q| = 0$ ) and parallel singularities ( $|J_x| = 0$ ). The former singularities arise from  $\{z|z = q_1\} \cup \{z|z = q_2\} \cup \{z|z = q_3\}$ , which implies  $L = R_b - R_n$ , by geometric expression; hence, it leads to  $R_b - R_n < L$ . The latter one arises from the constraint that three vectors  $(B_1 - A_1)^T$ ,  $(B_2 - A_2)^T$  and  $(B_3 - A_3)^T$  are coplanar. In summary, to eliminate this configuration, we can effectively avoid the singularities by imposing the following constraints:

$$R_b - R_n < L \quad (8)$$

$$0 < \Psi_i < \frac{\pi}{2}, \text{ for } i = 1, 2, 3$$

To determine the workspace of the robot, the intersection of the three kinematic chains has to be set forth. As the workspace of each kinematic chain is a sphere of radius  $L$  with center  $A_i(d \cos \alpha_i, d \sin \alpha_i, q_i)$ , the workspace of the robot is the set of the intersections of the three circles along a given  $q_i$  with radius  $R_{ci} = \sqrt{L^2 - (z - q_i)^2}$ . Inside this cylinder in Fig. 2, we can prescribe a parallelepiped of volume  $2r$  to obtain the regular dexterous workspace, where

$$r = \sqrt{(S_1 z + S_2)^2 + (N_1 z + N_2)^2} \quad (9)$$

The manipulability represents how easy the device can get operation speed in the link's range of interest and, it is expressed by the formulation of  $w = \sqrt{\det(J^T J)^{-1}}$  or  $w = |\det J^{-1}|$ . For this manipulator, we can infer that the value of the manipulability is proportional to  $d$ , especially in  $z$  direction to  $d^2$ . Because the manipulator contains only translational displacement, which is proportional to the manipulability, we can meet the range of motion along the  $z$  direction with no concern of the manipulability.

### B. Selections of actuator and sensor

We selected a voice coil motor a linear actuator that has sufficient stroke as well as sufficiently fast response up to 12Hz sinusoidal motion. Using the inverse kinematics (4), the stroke of each voice coil motor was determined by giving the constraints. The stroke was bounded as the mass and size of the coil because the magnetic flux depends on the size. Considering this, the AVR-19.5 (Motion Control Product Ltd.) having sufficiently long 5mm stroke, was selected according to the specifications of the actuator. A Mercury II™ 1600 (GSI MicroE Systems) linear encoder was selected to meet the requirements of a minimal positioning accuracy of 10 μm. The encoder is the incremental optical encoder, which detects the amount of light reflected from the scratched surface. The encoder gathers the light reflected and digitalizes the amount of light into the A and B phase with the 0.5 μm resolutions.

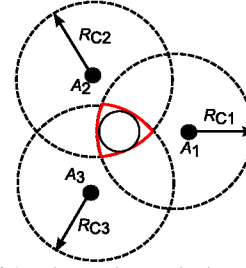


Fig. 2. Workspace of the Linear Delta manipulator [21]

### C. Design of the tremor suppression system

To construct the tremor suppression device, two parts of design – the actuating part and manipulating part – are needed.

First, the actuating part consists of three modules, and a module involves a voice coil motor, a high precision encoder, and a linear guide to generate three translational motions, as shown in Figs. 3(a)-(c). A linear guide with low friction enables accurate high-speed linear movement, and a small scale linear guide (WRG1020, Won ST, 3.8mm×4mm×20mm) was selected to connect the coil part of the voice coil motor. Since the mass of the magnetic part of the voice coil motor is larger than the coil part, the coil part was mounted on the main body of the fixed frame, as shown in Fig. 3 (a). Here, an upper support attached to the coil part was designed to make linearly move. The upper support was able to move together with one of the leg of the parallel manipulator, to be shown in Fig.4 (b). While, the lower support is attached to the fixed frame and the magnetic part of the voice coil motor. For an accurate and immediate transportation up to 12 Hz, the design has to be made so that two guides were attached in parallel for stable linear movement. In same manner, two pairs of additional modules were made, and these were placed in 120-degree intervals on the end plate holder. The end plate holder, as shown in Fig. 3 (e), supports these modules and helps the magnetic bar make the linear movement parallel to the linear guide under a certain friction with the magnetic bar. The fixing parts in Fig. 3 (f) were made to prevent the bending of each

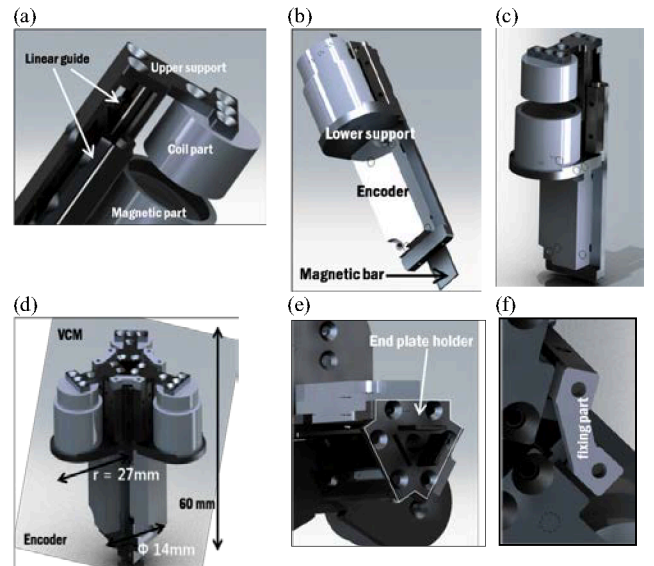


Fig. 3. The 3D modeling of the actuating module ((a) – (c)) and assembly of the module (d) with (e) end plate holder and (f) fixing part.

sub system with respect to the end plate. The full actuated system is shown in Fig. 3 (d). It has a hand grip with a minimum diameter of 14mm, height of 60mm, and maximum radius of 27mm.

On the other hand, the second manipulating part is to give the desired three-dimensional translational position to the end-effector of the manipulator. As the conventional spherical joint has the limitations of small size and high friction, the concept of the flexure joint [23]-[24] was introduced. The flexure joint allows bending and torsions and can reduce the inaccuracy compared to the conventional spherical joint. From such consideration, all twelve spherical joints in three kinematic chains were modeled as a wide range of flexure joints, in same manner in [24], as shown in Fig. 4 (a). Furthermore, for low-cost and easy fabrication, a manipulator was made by using the Rapid Prototype (RP) material of FullCure 720 (Objet Geometries, Ltd). As the material of RP is not rigid, unexpected overshoots of the actuator may cause damage. To avoid this, all flexure-based spherical joints may be modeled as a cylindrical bar with a radius of at least 0.8 mm. Finally, in order to avoid the singularities as mentioned earlier in (8), the main properties of the kinematic chain in Linear Delta manipulator, the length of linkage  $L$ , the radius of the mobile platform  $R_n$  and base platform  $R_b$  are chosen as  $9\text{ mm}$ ,  $5.5\text{ mm}$  and  $9\text{ mm}$ , respectively. From these considerations, the manipulating part is proposed, as shown in Fig. 4 (b).

The proposed parallel manipulator is attached to the actuating part which enables us to allow the base frame of the manipulator into three parallel vertical motions in Fig. 5. Combining those, it leads the tool tip to generate three translation motions. As the device has a resolution of  $0.5\ \mu\text{m}$

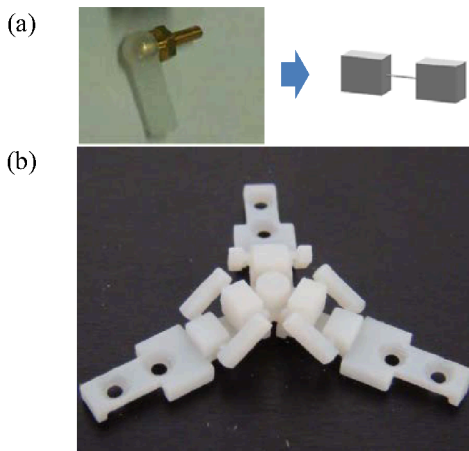


Fig. 4. (a) Consideration of the spherical joint into the flexure joint, (b) the proposed manipulator made by Rapid Prototype.

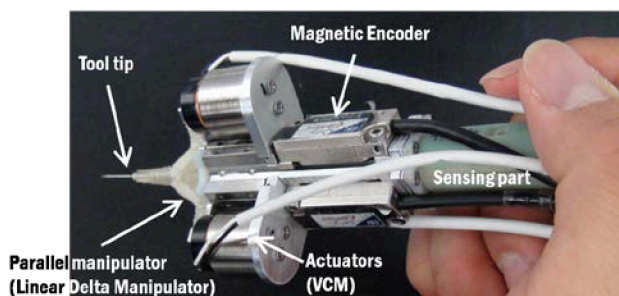


Fig. 5. Configuration of the system assembly.

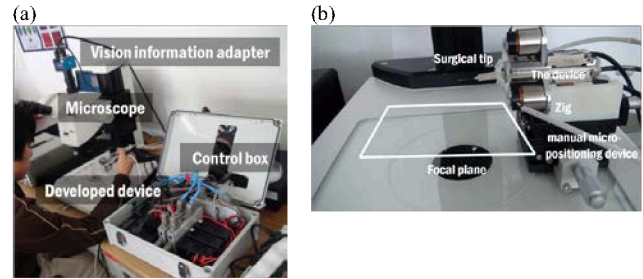


Fig. 6. (a) Experimental environments and (b) experimental setup

and maximum speed of  $20\text{ mm/s}$ , it can have an accuracy of  $1\ \mu\text{m}$  and an average speed of at least  $12\text{ mm/s}$ . The total size of the system is about  $10\text{ cm}$  in length and  $200\text{ g}$  in weight.

### III. EXPERIMENTS AND RESULTS

The goal of the experiments is to check whether or not it is possible to use the developed manipulator as a device for tremor suppression. In order to suppress the physiological tremor, although real microsurgical applications includes the technics of the anti-phase compensation of the tremor, it will be verified here that the desired values to be compensated in anti-phase can be appropriately controlled by the proposed system. It is essential to consider the control performance of the tracking the desired trajectory in terms of speed (rising time and frequency) and accuracy (to remove the control error).

At first, each of the voice coil motors have been controlled appropriately and then the end-effector has moved correctly 1) when its desired trajectories (two types: incremental steps, sine wave tracking) were given. Then, from the manipulator with three voice coil motors, 2) the end-effector has followed the desired trajectories (incremental steps in the  $x$  and  $z$  axes, sinusoidal signal in the  $z$  axis). The trajectory values of the desired position of the end-effector are modeled as the 5th polynomial and all position controls in all procedures were performed through the PID control. Also, all the movements of each actuator were measured by the encoder attached on the based frame and the magnetic bar.

Fig. 6. shows the experimental environments and the detailed configuration of the control box (the computer used for the experiments is not shown). The motor drive (Cello, Elmo Motion Control) and power supply are used to actuate the three voice coil motors. For all experiments, the MATLAB 2009Ra (Matworks Corporation) environment using MATLAB Simulink and Quarc Q8-USB board was used. All experiments were conducted on a PC running on an Intel® Core™ i7 3.70 GHz CPU and a Geforce GTX 570 graphic card. The DAQ components of the Quarc Q8-USB board (Quancer, Canada) consist of eight encoders, eight analog outputs, and eight analog inputs. In this study, to control each axis of the voice coil motors of the manipulator, three encoder signals were used. Finally, three analog outputs were used to provide the desired positions. All signals were sampled at a rate of  $1\text{ kHz}$  using this data acquisition board. For the following tests, as in Fig. 6(b), a microscope was used as a precise displacement sensor by means of visual processing of the focal plane. The manual micro-positioning device and jig



were used for precise movement of the base platform of the proposed manipulator.

In this study, simple experiments were conducted for characterizing the developed manipulator. On the other hand, the actual movement of each motor may exceed  $200\mu\text{m}$ , so the end-effector has to be moved, particularly in the z axis. Also, actual tremulous signal components include the rapid vibrations of 10Hz during the sine wave tracking. Considering these facts, the procedural steps of this study can be described as follows: Figs. 7 (a) and (b) represent the control performance of a single axis motor of the sub-system, respectively. In this figure, the desired position varies with incremental steps of  $50\mu\text{m}$ , and is given as the sinusoidal signal with an amplitude of  $500\mu\text{m}$  and a frequency of 10Hz. Although the desired position in each axis was not perfectly controlled, they had negligible delay below 2ms and roughly followed the value of the desired position. Therefore, robust position control using the voice coil motor was performed.

After these two tests, it was essential to check how well the desired position of the end-effector was followed. Three voice coil motors were confirmed to be properly controlled, where the end-effector of manipulator could move with respect to each desired position values. From the fact that the Linear Delta manipulator has a structure easily movable along the z direction and if the end-effector of the Linear Delta manipulator is only moving along the z direction, it is evident that the motors should all be controlled all equally along the z direction, as in Fig. 8(a). Similarly, the control performance along the x or y direction could be tested. The test would be sufficient for only the x direction in that the x and y directions in the workspace of Linear Delta manipulator appears symmetrically in Fig. 1. Each real movement of the motors

can be correlated with corresponding values calculated from the end-effector by means of the inverse kinematic model of the Linear Delta manipulator (4). The effector was forced to move with a certain step in the z axis and  $100\mu\text{m}$  in the x axis every step, respectively, as shown in Fig. 8 (b). Given  $100\mu\text{m}$  of the desired position in the axis, each actuator has to be moved  $40.8\mu\text{m}$ ,  $-21.4\mu\text{m}$ , and  $-21.4\mu\text{m}$  respectively in the z axis. Fig. 8(c), on the other hand, shows the response of the sine wave tracking. The frequency of the input signal was 8Hz and the amplitude was  $100\mu\text{m}$ . They had negligible delay but the results following the peak-to-peak were not perfect. The third motor had more control input for the same movement, which resulted from the friction between the end plate holder and the magnetic bar of the corresponding sub-system.

#### IV. DISCUSSION AND CONCLUSION

In this study, a new design of a parallel manipulator for the suppression of physiological hand tremor in the field of microsurgery has been proposed. For efficient compensation of tremor while performing microsurgery, a manipulator should meet the following requirements: sinusoidal waves fast as 8-12Hz in frequency, amplitudes of  $50\text{-}150\mu\text{m}$ , and an accuracy of  $10\mu\text{m}$ .

Therefore, for immediate and accurate tremor compensation, the voice coil motor was selected and the design of the new parallel manipulator for tremor canceling was proposed and finally the manipulator was developed. Tremor compensation using the Linear Delta parallel manipulator has several advantages. As it has the inherited the structural property of having relatively simple kinematics and Jacobian matrix, the numerical error can be reduced. Also, due to the fact that it has a relatively large workspace in the direction of movement in the z axis, it is applicable to insure

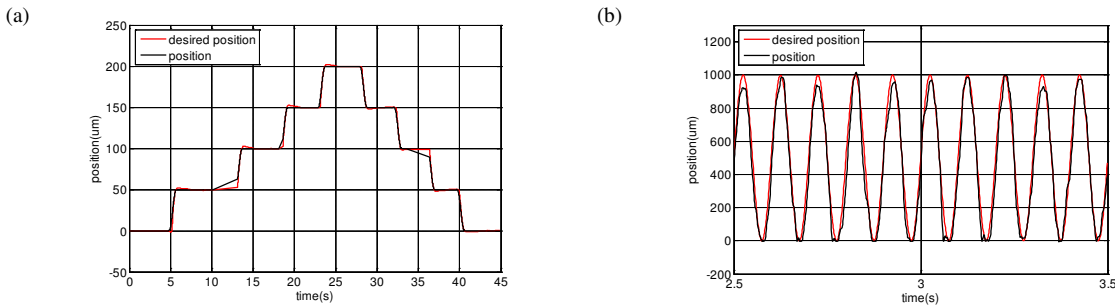


Fig. 7. The graphs of the current position (blue line) when the desired position (green line) is given as (a) an incremental step of  $50\mu\text{m}$  and (b) a sine wave with an amplitude of  $500\mu\text{m}$  and a frequency of 10Hz

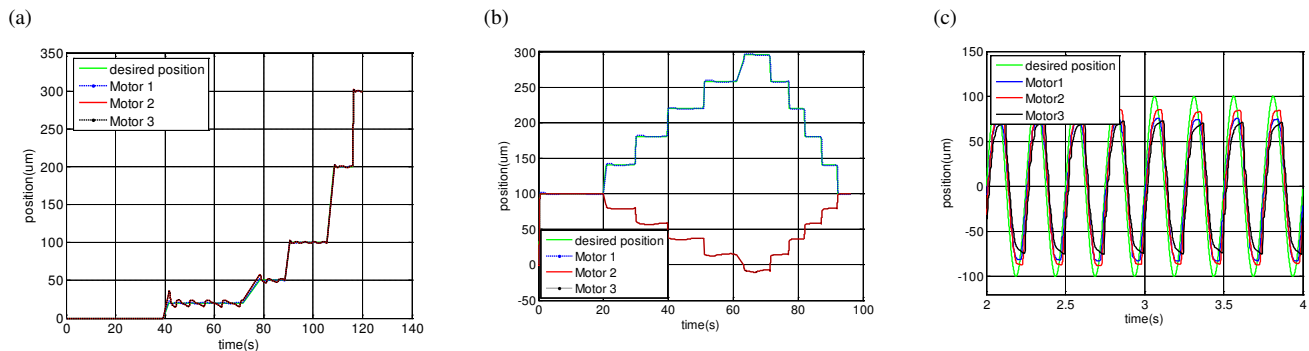


Fig. 8. The graphs of current position (Motor 1: blue line, Motor 2: red, Motor 3: yellow) when the desired position (green line) is given as (a) a certain incremental step in the z axis, (b) an incremental step of  $100\mu\text{m}$  in the x axis and (c) a sinusoidal signal with an amplitude of  $100\mu\text{m}$  and a frequency of 8Hz in the z axis.

the vetical mobility in microsurgery. Lastly, from the fact that it has no additional computation related to coordinate transformation, computational efficiency can be improved.

To validate the feasibility of the developed manipulator, simple experiments were performed using the microscope as a vision-based displacement sensor onto how well it tracks if given 1) the desired trajectory (for example, a rectangle with the length of one side of 200  $\mu\text{m}$ ) and 2) sine wave trajectory at the end-effector. The feasibility tests show promising results of the proposed manipulator in microsurgical applications for the compensation of tremor. In future work, to identify the movements of the end-effector of the manipulator, the microscope will be used as a precise displacement sensor, as shown in Fig. 9. The movement of the surgical needle attached to the end-effector of the device can be observed in the focal plane of the microscope in real time, and the sine wave tracking and chirp signal tracking should be performed further. While this study mainly focused on actuating part and manipulating part, the suppression experiments using the proposed device including the sensing part will finally be performed during the insertion task.

#### ACKNOWLEDGEMENT

This work was supported by the Center for Integrated Smart Sensors funded by the Ministry of Science, ICT & Future Planning as Global Frontier Project" (CISS-2012M3A6A6054195)

#### REFERENCES

- [1] Elble, R. and W. Koller, "Physiology of normal tremor," Tremor, The Hohns Hopkins University Press, Baltimore, 1990, pp 37-53.
- [2] Patkin, M., "Ergonomics applied to the practice of microsurgery," Australian and New Zealand Journal of Surgery, vol. 47, no. 3, pp 320-329, 1977.
- [3] Harwell, R. C. and R. L. Ferguson. "Physiologic tremor and microsurgery," Microsurgery, vol. 4, no.3, pp 187-192, 1983.
- [4] McAuley, J. and C. Marsden, "Physiological and pathological tremors and rhythmic central motor control," Brain, vol. 123, no. 8, pp 1545, 2000.
- [5] Nezhat C, Saberi NS, Shahmohamady B, Nezhat F, "Robotic-assisted laparoscopy in gynecological surgery", JLS, vol. 10, no. 3, pp. 317–320, Jul-Sep, 2006.
- [6] Nezhat C, Saberi NS, Shahmohamady B, Nezhat F, "Robotic-assisted laparoscopy in gynecological surgery", JLS, vol. 10, no. 3, pp. 317–320, Jul-Sep, 2006.
- [7] B. Mitchell, J. Koo, I. Iorcachita, P. Kazanzides, A. Kapoor, J. Handa, G. Hager, and R. Taylor, "Development and application of a new steadyhand manipulator for retinal surgery," in 2007 Proc. IEEE Int. Conf. Robot. Autom.(ICRA), pp. 623–629.
- [8] T. Ueta et al., "Robot-assisted vitreoretinal surgery: Development of a prototype and feasibility studies in an animal model," Ophthalmol., vol. 116, no. 8, pp. 1538–1543, 2009.
- [9] W. T. Ang, C. N. Riviere, and P. K. Khosla, "An active hand-held instrument for enhanced microsurgical accuracy," in Proc. MICCAI, vol. 1935, pp. 878-886, 2000.
- [10] C. N. Riviere, W. T. Ang, and P. K. Khosla, "Toward active tremor canceling in handheld microsurgical instruments," IEEE Trans. Rob. Autom., vol. 19, pp. 793–800, 2003.
- [11] B. C. Becker, "Vision-Based Control of a Handheld Micromanipulator for Robot-Assisted Retinal Surgery", Ph.D. dissertation, Carnegie Mellon University, Pittsburgh, Pennsylvania, USA, 2011.
- [12] B. C. Becker, C. R. Valdivieso, J. Biswas, L. A. Lobes, and C. N. Riviere, "Active guidance for laser retinal surgery with a handheld instrument," in 2009Proc.IEEE Int. Conf.Eng.Med.Biol. Soc.(EMBC), pp.5587-5590.
- [13] B. C. Becker, R. A. MacLachlan, L.A. Lobes, C. N. Riviere, "Semiautomated intraocular laser surgery using handheld instruments", Lasers Sur Med., vol. 42, pp264–273, 2010.
- [14] B. C. Becker, S. Voros, J. Louis, L.A. Lobes, JT. Handa, Hager GD, C.N. Riviere, "Retinal vessel annulation with an image-guided handheld robot," in 2010 Proc. IEEE Int. Conf. Eng. Med. Biol.Soc.(EMBC), pp5420–5423.
- [15] B. C. Becker, R. A. MacLachlan, L.A. Lobes, C. N. Riviere, "Vision-based retinal membrane peeling with a handheld robot," in 2012 Proc. IEEE Int. Conf. Robot. Autom.(ICRA), pp.1075-1080.
- [16] Win Tun Latt; Newton, R.C.; Visentini-Scarzanella, M.; Payne, C.J.; Noonan, D.P.; Jianzhong Shang; Guang-Zhong Yang, "A Hand-held Instrument to Maintain Steady Tissue Contact during Probe-Based Confocal Laser Endomicroscopy," IEEE Transactions on Biom. Eng., vol.58, no.9, pp.2694-2703, Sept. 2011.
- [17] W. T. Latt, U. X. Tan, C.Y. Shee, andW. T. Ang, "A compact hand-held active physiological tremor compensation instrument," in 2009 Proc. IEEE/Amer.Soc. Mech. Eng. Int. Conf. Adv. Intell. Mechatronics, pp. 711–716, 2009.
- [18] J.C. Tabar s, R.A. MacLachlan, C.A. Etensohn, C.N. Riviere, "Cell micromanipulation with an active handheld micromanipulator," in Proc. IEEE Int. Conf. Eng. Med. Biol. Soc., pp.4363-4366, 2010.
- [19] R. A. MacLachlan, B. C. Becker, J. Cuevas Tabares, G. W. Podnar, L. A. Lobes Jr., and C. N. Riviere, "Micron: An actively stabilized handheld tool for microsurgery," IEEE Trans. Rob., vol. 28, no. 1, pp.195-212, 2012.
- [20] O.Company, F. Pierrot, Modeling and design issues of a 3-axis parallel machine-tools, Mechanism and Machine Theory, vol. 37, pp.1325-1345, 2002.
- [21] R. Kelaiaia, O. Company and A. Zaatri, "Multi objective optimization of a linear Delta parallel robot", Mechanism and Machine Theory, vol. 50, pp.159-178, 2012.
- [22] Liu, Xin-Jun and Wang, Jinsong and Oh, Kun-Ku and Kim, Jongwon, "A New Approach to the Design of a DELTA Robot with a Desired Workspace", Journal of Intelligent & Robotic Systems, vol. 39, no. 2, pp.209-225, 2004.
- [23] M. Bouri, R. Clavel, "The Linear Delta: Developments and Applications," Robotics (ISR), 2010 41st Int. Symposium on and 6th German Conference on Robotics (ROBOTIK) , vol., no., pp.1-8, 2010
- [24] Wei Dong, Zhijiang Du, Lining Sun, "Conceptional Design and Kinematics Modeling of a Wide-Range Flexure Hinge-Based Parallel Manipulator", in Proc. IEEE Int. Conf. Robot. Autom.(ICRA),pp.4031-4036, 2005.
- [25] Wei Dong; Zhijiang Du; Lining Sun, "Stiffness influence atlases of a novel flexure hinge-based parallel mechanism with large workspace," in Proc. IEEE/RSJ Int. Conf. on Intelligent Robots and Systems (IROS), pp.856-861, 2005